

Analytical validity of nanopore sequencing for rapid SARS-CoV-2 genome analysis

Rowena A. Bull^{1,2*}, Thiruni Adikari^{1,2*}, James M. Ferguson³, Jillian M. Hammond³, Igor Stevanovski³, Alicia G. Beukers⁴, Zin Naing^{2,5}, Malinna Yeang^{2,5}, Andrey Verich¹, Hasindu Gamaarachchi^{3,6}, Ki Wook Kim^{2,5}, Fabio Luciani^{1,2}, Sacha Stelzer-Braide^{2,5}, John-Sebastian Eden^{7,8}, William D. Rawlinson^{2,5,9,10}, Sebastiaan J. van Hal^{4,11} & Ira W. Deveson^{3,12#}

* These authors contributed equally.

Correspondence: i.deveson@garvan.org.au

¹The Kirby Institute for Infection and Immunity, University of New South Wales, Sydney, NSW, Australia.

²School of Medical Sciences, Faculty of Medicine, University of New South Wales, Sydney, NSW, Australia.

³Kinghorn Centre for Clinical Genomics, Garvan Institute of Medical Research, Sydney, NSW, Australia.

⁴NSW Health Pathology, Department of Infectious Diseases and Microbiology, Royal Prince Alfred Hospital, Sydney, NSW, Australia.

⁵Virology Research Laboratory, Serology and Virology Division (SAViD), NSW Health Pathology, Prince of Wales Hospital, Sydney, NSW, Australia.

⁶School of Computer Science and Engineering, University of New South Wales, Sydney, NSW, Australia.

⁷Marie Bashir Institute for Infectious Diseases and Biosecurity & Sydney Medical School, The University of Sydney, Sydney, NSW, Australia

⁸Centre for Virus Research, Westmead Institute for Medical Research, Sydney, NSW, Australia

⁹School of Women's and Children's Health, Faculty of Medicine, University of New South Wales, Sydney, NSW, Australia.

¹⁰School of Biotechnology and Biomolecular Sciences, Faculty of Science, University of New South Wales, Sydney, NSW, Australia.

¹¹Central Clinical School, University of Sydney, Sydney, NSW, Australia.

¹²St Vincent's Clinical School, Faculty of Medicine, University of New South Wales, Sydney, NSW, Australia.

ABSTRACT

Viral whole-genome sequencing (WGS) provides critical insight into the transmission and evolution of Severe Acute Respiratory Syndrome Coronavirus 2 (SARS-CoV-2). Long-read sequencing devices from Oxford Nanopore Technologies (ONT) promise significant improvements in turnaround time, portability and cost, compared to established short-read sequencing platforms for viral WGS (e.g., Illumina). However, adoption of ONT sequencing for SARS-CoV-2 surveillance has been limited due to common concerns around sequencing accuracy. To address this, we performed viral WGS with ONT and Illumina platforms on 157 matched SARS-CoV-2-positive patient specimens and synthetic RNA controls, enabling rigorous evaluation of analytical performance. Despite the elevated error rates observed in ONT sequencing reads, highly accurate consensus-level sequence determination was achieved, with single nucleotide variants (SNVs) detected at >99% sensitivity and >99% precision above a minimum ~60-fold coverage depth, thereby ensuring suitability for SARS-CoV-2 genome analysis. ONT sequencing also identified a surprising diversity of structural variation within SARS-CoV-2 specimens that were supported by evidence from short-read sequencing on matched samples. However, ONT sequencing failed to accurately detect short indels and variants at low read-count frequencies. This systematic evaluation of analytical performance for SARS-CoV-2 WGS will facilitate widespread adoption of ONT sequencing within local, national and international COVID-19 public health initiatives.

INTRODUCTION

Severe Acute Respiratory Syndrome Coronavirus 2 (SARS-CoV-2) is the causative pathogen for COVID-19 disease^{1,2}. SARS-CoV-2 is a positive-sense single-stranded RNA virus with a ~30 kb poly-adenylated genome^{1,2}. Complete genome sequences published in January 2020^{1,3} enabled development of RT-PCR assays for SARS-CoV-2 detection that have served as the diagnostic standard during the ongoing COVID-19 pandemic⁴.

Whole-genome sequencing (WGS) of SARS-CoV-2 provides additional data to complement routine diagnostic testing. Viral WGS informs public health responses by defining the phylogenetic structure of disease outbreaks⁵. Integration with epidemiological data identifies transmission networks and can infer the origin of unknown cases⁶⁻¹¹. Large-scale, longitudinal surveillance by viral WGS may also provide insights into virus evolution, with important implications for vaccine development¹²⁻¹⁵.

WGS can be performed via PCR amplification or hybrid-capture of the reverse-transcribed SARS-CoV-2 genome sequence, followed by high-throughput sequencing. Short-read sequencing technologies (e.g., Illumina) enable accurate sequence determination and are the current standard for pathogen genomics. However, long-read sequencing devices from Oxford Nanopore Technologies (ONT) offer an alternative with several advantages. ONT devices are portable, cheap, require minimal supporting laboratory infrastructure or technical expertise for sample preparation, and can be used to perform rapid sequencing analysis with flexible scalability¹⁶.

The use of ONT devices for viral surveillance has been demonstrated during Ebola, Zika and other disease outbreaks¹⁷⁻¹⁹. Although protocols for ONT sequencing of SARS-CoV-2 have been established and applied in both research and public health settings²⁰⁻²², adoption of the technology has been limited due to concerns around its accuracy. ONT devices exhibit lower read-level sequencing accuracy than short-read platforms²³⁻²⁵. This may have a disproportionate impact on SARS-CoV-2 analysis, due to the virus' low mutation rate (8×10^{-4} substitutions per site per year²⁶), which ensures erroneous (false-positive) or undetected (false-negative) genetic variants have a strong confounding effect.

In order to address concerns regarding ONT sequencing accuracy and evaluate its analytical validity for SARS-CoV-2 genomics, we have performed amplicon-based nanopore and short-read WGS on matched SARS-CoV-2-positive patient specimens and synthetic RNA controls, allowing rigorous evaluation of ONT performance characteristics.

RESULTS

Analysis of synthetic SARS-CoV-2 controls

Synthetic DNA or RNA reference standards can be used to assess the accuracy and reproducibility of next-generation sequencing assays²⁷. We first sequenced synthetic RNA controls that were generated by *in vitro* transcription of the SARS-CoV-2 genome sequence. The controls matched the Wuhan-Hu-1 reference strain at all positions, allowing analytical errors to be unambiguously identified. To mimic a real-world viral WGS experiment, synthetic RNA was reverse-transcribed then amplified using multiplexed PCR of $98 \times$ ~400 bp amplicons that enabled evaluation of ~95% of the SARS-CoV-2 genome. Eight independent replicates were sequenced on ONT PromethION and Illumina MiSeq instruments (see **Methods**).

We aligned the resulting reads to the Wuhan-Hu-1 reference genome to assess sequencing accuracy and related quality metrics (**Fig. S1a-i**). Illumina and ONT platforms exhibited distinct read-level error profiles, with the latter characterised by an elevated rate of both substitution (23-fold) and insertion-deletion (indel) errors (76-fold; **Table 1**; **Fig. S1d,e**). Per-base error frequency profiles showed clear correlation between ONT replicates (substitution $R^2 = 0.67$; indel $R^2 = 0.82$; **Fig. S1f,g**). This indicates that ONT sequencing errors are not entirely random but are influenced by local sequence context. For example, indel errors were enriched (1.4-fold) at low-complexity sequences within the SARS-CoV-2 genome (i.e., sites with homopolymeric or repetitive content; ~1% of the genome; **Fig. S1d**). Illumina error profiles showed weaker correlation between replicates (substitution $R^2 = 0.15$; indel $R^2 = 0.42$), indicating that short-read sequencing errors were less systematic than for ONT libraries (**Fig. S1h,i**).

Despite their distinct error profiles, both sequencing platforms demonstrated high consensus-level sequencing accuracy across the SARS-CoV-2 genome. We used *iVar* and *Medaka* workflows to determine consensus genome sequences for Illumina and ONT libraries, respectively (see **Methods**). We detected just two erroneous variant candidates in a single ONT library (**Table 1**). Both of these were single-base insertions occurring at low-complexity sites (**Fig. S2**), with no erroneous SNVs detected in any replicate ($n = 8$). All Illumina libraries exhibited perfect accuracy (**Table 1**). Therefore, the sequencing artefacts affecting both technologies had minimal impact on the accuracy of consensus-level sequence determination, with indel errors in ONT samples being a possible exception.

Analysis of matched patient isolates

To further evaluate the suitability of ONT sequencing for SARS-CoV-2 genomics, we conducted rigorous proficiency testing using *bona fide* clinical specimens. We performed ONT and Illumina WGS on matched, de-identified SARS-CoV-2-positive cases collected at public hospital laboratories in Eastern & Southern New South Wales and Metropolitan Sydney from March-April 2020 (see **Methods**; **Supplementary Table 1**). The SARS-CoV-2 genome was enriched by PCR amplification, using a custom set of $14 \times \sim 2.5$ kb amplicons that covers 29783/29903 bp (99.6%) of the genome, including 100% of annotated protein-coding positions⁶. Pooled amplicons then underwent parallel library preparation and sequencing on an ONT GridION/PromethION and an Illumina MiSeq instrument (see **Methods**). Short-read sequencing was performed according to a pathogen genomics accredited diagnostic workflow in a reference NSW Health Pathology laboratory, enabling direct comparison of nanopore sequencing to the established standard for pathogen genomics.

In total, we obtained complete (99.6%) genome coverage with both technologies for 157 matched positive cases (**Supplementary Table 1**). By comparison to the Wuhan-Hu-1 reference strain, Illumina sequencing identified 7.6 consensus single-nucleotide variants (SNVs) and 0.04 indels, on average, per sample. A further 1.0 SNVs and 0.2 indels per sample were detected at sub-consensus read-count frequencies (20 – 80%), indicative of intra-specimen genetic diversity (see below). Excluding positions with evidence of sub-consensus variation, this provides an overall comparison set of 1201 consensus variants and 4,674,554 positions that match the reference strain in a given sample, against which to assess the accuracy of SARS-CoV-2 nanopore sequencing (**Supplementary Table 1**).

We used each of two best-practice bioinformatics pipelines developed by the ARTIC network to identify consensus variants with ONT sequencing data. The alternative pipelines differed primarily in their use of either *Medaka* or *Nanopolish* to call variants (see **Methods**). In general, ONT variant candidates identified by both pipelines were highly concordant with the Illumina comparison set. Illumina variants were detected with 99.17% sensitivity and 99.58% precision by *Nanopolish*, compared to 98.33% sensitivity and 99.24% precision by *Medaka* (**Table 2**). Undetected variants (false-negatives) were more frequent than erroneous candidates (false-positives), occurring in 14/157 (9%) and 9/157 (6%) of *Medaka* samples, respectively (**Supplementary Table 2**). Only 1/7 (14%) of consensus indels in the Illumina comparison set was detected by either *Nanopolish* or *Medaka*, while a further five and nine false-positive indels were detected by the respective pipelines (**Supplementary Table 2**). While the scarcity of consensus indels detected with either sequencing technology prevented a more thorough evaluation of indel accuracy, this indicates that ONT is inadequate for accurate detection of small indels in the SARS-CoV-2 genome. In contrast, SNVs were detected by *Nanopolish* and *Medaka* with high accuracy: overall, we found 99.66% and 98.83% concordance between ONT and Illumina SNVs, as measured by Jaccard similarity, with identical results in 145/157 (92%) and 153/157 samples (97%), respectively (**Table 2**).

Inspection of false-positive and false-negative variant candidates detected with ONT sequencing data showed that these tended to occur in low-complexity sequences, which are known to be refractory to ONT base-calling algorithms²³. For example, false-negative and/or false-positive candidates were found within a 21 bp T-rich site in the *orf1ab* gene in multiple samples (**Fig. S3a,b**). We identified fifteen problematic low-complexity sites in the SARS-CoV-2 genome ranging in size from 9 to 42 bp in length that showed elevated read-level sequencing error rates (**Fig. S1d; Supplementary File 1**). Exclusion of these positions (~1% of the genome) improved the fidelity of ONT variant detection, with consensus SNVs in the Illumina comparison set being detected with 99.83% and 99.40% sensitivity by *Nanopolish* and *Medaka*, respectively, and perfect

precision for both. Consensus SNVs detected with the *Nanopolish* workflow were identical between ONT and Illumina data in 155/157 (99%) of samples (**Table 2**; **Supplementary Table 3**). This suggests that the accuracy of nanopore WGS may be improved via the exclusion of a small number of ‘blacklist’ low-complexity sites in the SARS-CoV-2 genome from downstream analysis.

We next assessed the impact of sequencing depth on ONT performance. To do so, we down-sampled nanopore sequencing reads from a uniform 200-fold coverage across the SARS-CoV-2 genome and repeated variant detection across a range of coverage depths (see **Methods**). Both sensitivity and precision of variant detection were strongly influenced by sequencing coverage, showing a sharp decline below ~50-fold coverage depth, with minimal improvement observed above ~60-fold (**Fig. 1a,b**). As above, excluding error-prone low-complexity sequences afforded consistent improvements to sensitivity and overall concordance across the range of depths tested (**Fig. 1a,b**).

To verify these observations and assess reproducibility, we re-sequenced twelve specimens to generate triplicate ($n = 3$) data on both Illumina and ONT platforms (see **Methods**). We measured reproducibility by performing pairwise comparisons of detected variant candidates between replicates for a given sample (**Supplementary Table 4**). No discordant variants were detected between Illumina replicates across any of the 36 pairwise sample comparisons (309 variants total), confirming the reliability of short-read WGS. ONT also showed high reproducibility, with 99.36% Jaccard similarity between *Medaka* replicates for consensus variants (310 total) and perfect concordance for SNVs (**Supplementary Table 4**).

In summary, ONT sequencing enabled highly accurate and reproducible detection of consensus-level SNVs in SARS-CoV-2 patient isolates but appears generally unsuitable for the detection of small indel variants.

Detection of intra-specimen variation

Within-host genetic diversity is a common feature of RNA viruses, with divergent quasi-species present in a single infection. Within-host diversity may help infecting viruses evade the host immune response, adapt to changing environments and can cause more severe and/or long-lasting disease²⁸⁻³⁰. Resolving this diversity may also better inform studies of virus transmission than consensus-level phylogenetics alone³¹⁻³³. Therefore, we next evaluated the capacity of nanopore sequencing to identify intra-specimen genetic variation by detecting variants present at sub-consensus frequencies (i.e. variants detected in < 80% of mapped reads). Analysis of the SARS-CoV-2 synthetic RNA controls (see above) showed that sequencing artefacts in Illumina libraries could be misinterpreted as variants at read-count frequencies below ~20% (**Fig. S2b**), effectively establishing a lower bound for variant detection. We therefore limited our analysis to variants detected at $\geq 20\%$ frequency, taking variants detected by Illumina sequencing above this level to be genuine. Overall, short-read sequencing identified sub-consensus variants (20-80%) in 54/157 samples, comprising 156 SNVs and 20 indels (**Supplementary Table 5**).

Using *Varscan2*, we identified 154 sub-consensus SNV candidates in ONT sequencing libraries (**Supplementary Table 5**). We detected 119 SNVs (sensitivity = 76.3%) in the Illumina comparison set and 25 false-positives (precision = 82.6%; **Supplementary Table 5**). Read-count frequencies for variants identified with both technologies were correlated ($R^2 = 0.69$), indicating that these were *bona fide* variants, rather than sequencing artefacts (**Fig. 1c**). While the overall performance of sub-consensus SNV detection was quite poor, most false-positives and false-negatives were confined to the lower end of the frequency range assessed here (**Fig. 1c,d**). For example, SNVs at high (60-80%) and intermediate (40-60%) sub-consensus frequencies were detected with relatively high sensitivity (95.7%, 91.3%) and precision (100%, 97.7%), whereas low-frequency variants (20-40%) were detected with low sensitivity (63.2%) and precision (69.6%; **Fig. 1d**). Unsurprisingly, the high rate of indel errors in ONT sequencing libraries meant that they were unsuitable for detecting indel diversity, with errors overwhelming true variants (**Supplementary Table 5**).

In summary, ONT sequencing enabled detection of within-specimen SNVs at frequencies from ~40-80% with adequate accuracy but was generally unsuitable for the detection of indels or rare SNVs (< 40%).

Detection of structural variation

Large genomic deletions or rearrangements can have a major impact on virus function and evolution, however, there are currently just a few reported cases of SARS-CoV-2 specimens harbouring structural

variants (SVs)^{15,34}. Therefore, we next evaluated the detection of SVs in SARS-CoV-2 specimens with ONT sequencing. We used *NGMLR-Sniffles* to identify potential SVs in ONT libraries and validated these with supporting evidence from short-read sequencing (see **Methods**).

Across all SARS-CoV-2 patient specimens, we detected sixteen candidate deletions ranging in size from 15-1,840 bp (**Table 3**), while no other SV types were identified. Of these, 13/16 were supported by split short-read alignments and/or discordant read-pairs in matched Illumina libraries (**Fig. S4a; Table 3**). For 7/16 candidates, short-read evidence confirmed the presence of the deletion but indicated that the breakpoint position was not accurately placed by ONT reads (**Fig. S4b; Table 3**). Among the thirteen deletions detected by both platforms were examples in genes *S*, *M*, *N*, *ORF3*, *ORF6*, *ORF8* and *orf1ab* (**Table 3**). Only one variant, a 328 bp deletion in *ORF8* (**Fig. S4c**), was detected in multiple specimens, although highly similar (but not identical) 28 bp and 29 bp deletions were also detected in *S* in two unrelated specimens (**Fig. S4d**).

Overall, this analysis demonstrates that large deletions can be reliably detected using ONT sequencing and suggests that structural variation in the SARS-CoV-2 genome is more common and diverse than currently appreciated.

DISCUSSION

Viral WGS can be used to study the transmission and evolution of SARS-CoV-2, and is increasingly recognised as a critical tool for public health responses to COVID-19. Nanopore sequencing offers an alternative to established short-read platforms for viral WGS with several advantages. ONT devices: (i) are relatively inexpensive, highly portable and require minimal associated laboratory infrastructure; (ii) enable rapid generation of sequencing data and even real-time data analysis; (iii) require comparatively simple procedures for library preparation and; (iv) offer flexibility in sample throughput, accommodating single (e.g., Flongle), multiple (e.g., MinION/GridION) or tens/hundreds (e.g., PromethION) of specimens per flow-cell^{16,18}. Therefore, ONT sequencing could further empower SARS-CoV-2 surveillance initiatives by enabling point-of-care WGS analysis and improved turnaround time for critical cases, particularly in isolated or poorly resourced settings³⁵.

Due to the relatively low mutation rate observed in SARS-CoV-2²⁶, accurate sequence determination is vital to correctly define the phylogenetic structure of disease outbreaks. With ONT sequencing known to exhibit higher read-level sequencing error rates than short-read technologies²³⁻²⁵, reasonable concerns exist about suitability of the technology for SARS-CoV-2 genomics. Moreover, public databases for SARS-CoV-2 data (e.g., GISAID: <https://www.gisaid.org/>) already contain consensus genome sequences generated via ONT sequencing, potentially confounding investigations that rely on these resources.

The present study resolves these concerns, demonstrating accurate consensus-level SARS-CoV-2 sequence determination with ONT data. We report that: (i) variants at consensus-level read-count frequencies (80-100%) were detected with >99% sensitivity and >99% precision across 157 SARS-CoV-2-positive specimens, confirming the suitability of ONT sequencing for standard phylogenetic analyses; (ii) high accuracy and reproducibly was achieved by each of two alternative tools for ONT variant detection, with *Nanopolish* showing modest improvements over *Medaka*; (iii) a minimum ~60-fold sequencing depth was required to ensure accurate detection of SNVs, but little or no improvement was achieved above this level; (iv) false-positive and false-negative variants were typically observed at low-complexity sequences, with fidelity improved by excluding these problematic sites; (v) in contrast to consensus SNVs, ONT sequencing performed poorly in the detection of consensus indels or low-frequency variants (such variants should therefore be interpreted with caution); (vi) while the high indel error rate in ONT sequencing impedes accurate detection of small indels, long nanopore reads appear well-suited for the detection of large deletions and potentially other structural variants. Although SNVs alone are sufficient for routine phylogenetic analysis, small indels and large structural variants can profoundly impact gene function and are, therefore, of interest to studies of virus evolution and pathogenicity¹⁵.

As the first systematic evaluation of nanopore sequencing for SARS-CoV-2 WGS, this study removes an important barrier to its widespread adoption in the ongoing COVID-19 pandemic. While short-read sequencing platforms remain the gold-standard for high-throughput viral sequencing, the advantages to

portability, cost and turnaround-time afforded by nanopore sequencing imply that this emerging technology can serve an important complementary role in local, national and international COVID-19 response strategies.

MATERIALS & METHODS

Synthetic RNA controls

Synthetic controls used in this study were manufactured by Twist Biosciences and are commercially available (Catalog item 101024). The controls comprise synthetic RNA generated by *in vitro* transcription (IVT) of the SARS-CoV-2 genome sequence, representing the complete genome in $6 \times \sim 5$ kb continuous sequences. The controls used in this study are identical in sequence to the Wuhan-Hu-1 reference strain (MN908947.3), allowing sequencing artefacts to be readily identified. Synthetic controls were prepared for sequencing via a protocol established by the ARTIC network for viral surveillance (<https://artic.network/ncov-2019>). Briefly, reverse-transcription was performed on aliquots of synthetic RNA (at 10^6 copies per μL) using Superscript IV (Thermo Fisher Scientific) with both random hexamers and oligo-dT primers. Prepared cDNA was then amplified using multiplexed PCR with $98 \times \sim 400$ bp amplicons tiling the SARS-CoV-2 genome (ARTIC V3 primer set). Amplification was performed with Q5 Hotstart DNA Polymerase (New England Biolabs) with 1.5 μL of cDNA per reaction. PCR products were cleaned using AMPure XP beads (0.8X bead ratio), quantified using a Qubit fluorometer (Thermo Fisher Scientific) and partitioned into separate aliquots for analysis by short-read and nanopore sequencing. We note that it is not possible to amplify the entire SARS-CoV-2 genome in this way, since amplicons that span boundaries of the $6 \times \sim 5$ kb IVT products necessarily fail. Nevertheless, we were able to evaluate $\sim 95\%$ of the SARS-CoV-2 genome sequence.

SARS-CoV-2 specimens

SARS-CoV-2-positive extracts from 157 cases, tested at NSW Health Pathology East Serology and Virology Division (SaViD), were retrieved from storage and included in this study. All specimens were nasopharyngeal swabs originating from patients in New South Wales during March-April 2020. Specimens underwent total nucleic acid extraction using the Roche MagNA Pure DNA and total NA kit on an automated extraction instrument (MagNA pure 96). Reverse-transcription was performed on viral RNA extracts using Superscript IV VILO Master Mix (Thermo Fisher), which contains both random hexamers and oligo-dT primers. Prepared cDNA was then amplified separately with each of $14 \times \sim 2.5$ kb amplicons tiling the SARS-CoV-2 genome, as described elsewhere⁶. Amplification was performed with Platinum SuperFi Green PCR Mastermix (Thermo Fisher) with 1.5 μL of cDNA per reaction. PCR products were cleaned using AMPure XP beads (0.8X bead ratio), quantified using PicoGreen dsDNA Assay (Thermo Fisher). All $14 \times$ amplicon products from a given sample were then pooled at equal abundance and partitioned into separate aliquots for analysis by short-read and nanopore sequencing. This strategy ensured that any sequence artefacts potentially introduced during reverse-transcription and/or PCR amplification were common to matched ONT/Illumina samples, so would not be interpreted as false-positive/negatives during technology comparison.

Short-read sequencing

Pooled amplicons were prepped for short-read sequencing using the Illumina DNA Prep Kit, according to the manufacturer's protocol. Samples were multiplexed using Nextera DNA CD Indexes and sequenced on an Illumina MiSeq. Within each sequencing lane, a blank sample was also prepared and sequenced, in order to monitor for contamination and/or index swapping between samples. The resulting reads were aligned to the Wuhan-Hu-1 reference genome (MN908947.3) using bwa mem (0.7.12-r1039)³⁶. Primer sequences were trimmed from the termini of read alignments using iVar (1.0)³⁷. Trimmed alignments were converted to pileup format using samtools mpileup (v1.9)³⁸, with anomalous read pairs retained (--count-orphans), base alignment quality disabled (--no-BAQ) and all bases considered, regardless of PHRED quality (--min-BQ 0). Variants were identified using bcftools call (v1.9)³⁸, assuming a ploidy of 1 (--ploidy 1), then filtered for a minimum read depth of 30 and minimum quality of 20. Variants were classified according to their read-count frequencies as consensus (>80% reads supporting the variant) or sub-consensus (20-80%) variants, with the

latter further divided into high (60-80%), intermediate (40-60%) or low-frequency (20-40%). Variants at read-count frequencies below 20% were considered to be potentially spurious and excluded on this basis.

Nanopore sequencing

ARTIC amplicons (~400 bp) from the synthetic RNA controls were prepared for nanopore using the ONT Native Barcoding Expansion kit (EXP-NBD104). The longer amplicons (~2.5 kb) used on SARS-CoV-2 patient specimens were prepared for nanopore sequencing using the ONT Rapid Barcoding Kit (SQK-RBK004). Both kits were used according to the manufacturer's protocol. Up to twelve samples were multiplexed on a FLO-FLG001, FLO-MIN106D or FLO-PRO002 or flow-cell and sequenced on a GridION X5 or PromethION P24 device, respectively. In addition, a no-template negative control from the PCR amplification step was prepared in parallel and sequenced on each flow-cell (**Supplementary Table 6**). The *RAMPART* software package³⁹ was used to monitor sequencing performance in real-time, with runs proceeding until a minimum ~200-fold coverage was achieved across all amplicons. At this point, the run was terminated and the flow-cell washed using the ONT Flow Cell Wash kit (EXP-WSH003), allowing re-use in subsequent runs.

The resulting reads were basecalled using *Guppy* (4.0.14) and aligned to the Wuhan-Hu-1 reference genome (MN908947.3) using *minimap2* (2.17-r941)⁴⁰. The ARTIC tool *align_trim* was used to trim primer sequences from the termini of read alignments and cap sequencing depth at a maximum of 400-fold coverage. Consensus-level variant candidates were identified using each of two workflows developed by ARTIC (<https://github.com/artic-network/artic-ncov2019>), using *Nanopolish*⁴¹ or *Medaka* (0.11.5) to variants, respectively. *Nanopolish* variants candidates were filtered directly with the ARTIC *artic_vcf_filter* tool, while *Medaka* candidates were evaluated by *LongShot* (0.4.1)⁴² before filtering. Sub-consensus level variant candidates were identified using *Varscan2* (v2.4.3)⁴³.

Performance evaluation

For synthetic RNA controls, read-level quality metrics, such as sequencing error rates, were derived from read alignments using *pysamstats*, with any bases that differed from the Wuhan-Hu-1 reference sequence considered errors.

The accuracy of variant detection by ONT sequencing was evaluated by comparison to the set of variants identified by Illumina sequencing in matched cases. To ensure consistent representation of variants across calls generated by different programs: (i) multi-allelic variant candidates were separate into individual SNVs/indels using *bcftools norm* (1.9)³⁸; (ii) multi-nucleotide variants were decomposed into their simplest set of individual components using *rtg-tools vcfdecompose* (3.10.1) and; (iii) indels at simple repeats were left-aligned using *gatk LeftAlignAndTrimVariants* (4.0.11.0). Variant candidates identified by Illumina/ONT could then be considered concordant based on matching genome position, reference base and alternative base/s. For a given case, variant candidates identified with ONT and Illumina were classified as true-positives (TPs), candidates identified by ONT but not Illumina as false-positives (FPs) and candidates identified by Illumina but not ONT as false-negatives (FNs). The following statistical definitions were used to evaluate results:

$$\text{Sensitivity} = \text{TP} / (\text{TP} + \text{FN})$$

$$\text{Precision} = \text{TP} / (\text{TP} + \text{FP})$$

$$\text{Jaccard similarity} = \text{TP} / (\text{TP} + \text{FP} + \text{FN})$$

Structural variation

To identify structural variation, nanopore reads were re-aligned to the Wuhan-Hu-1 reference genome (MN908947.3) using the rearrangement-aware aligner *NGMLR* (v0.2.7)⁴⁴. *Sniffles* (v1.0.11)⁴⁴ was then used to detect candidate variants with a minimum length of 10 bp and ≥ 20 supporting reads. To validate SVs detected with ONT alignments, split short-read alignments and discordant read-pairs were extracted from matched Illumina libraries using *lumpy*⁴⁵. Variant candidates were then manually inspected to verify evidence from ONT and short-reads and assess break-point position resolution.

CODE AVAILABILITY

Software used in this study is generally open source and all publicly available. Full descriptions, including parameters and version numbers are provided in the **Materials & Methods** section, and further detail on the bioinformatics protocols can be found at: https://github.com/Psy-Fer/SARS-CoV-2_GTG

DATA AVAILABILITY

Raw data for SARS-CoV-2 whole genome sequencing experiments (ONT and Illumina) have been deposited to the Sequence Read Archive under Bioproject PRJNA651152.

ACKNOWLEDGEMENTS

We acknowledge the following funding support: UNSW COVID-19 Rapid Response Research Initiative (to W.D.R.), MRFF Investigator Grant APP1173594, Cancer Institute NSW Early Career Fellowship 2018/ECF013 and philanthropic support from The Kinghorn Foundation (to I.W.D.).

AUTHOR CONTRIBUTIONS

Z.N., M.Y., K.W.K., S.S.B., W.D.R. & S.J.vH. oversaw collection and handling of SARS-CoV-2 specimens.
T.A., A.V. & I.S. performed cDNA synthesis and PCR amplification of SARS-CoV-2 samples.
J.M.H. & I.S. performed ONT library preparation and sequencing.
A.G.B. performed Illumina library preparation and sequencing.
J.M.F., H.G., I.S., S.J.vH. & I.W.D. performed bioinformatics analysis.
I.W.D. prepared the figures.
R.A.B., W.D.R., S.J.vH., & I.W.D. prepared the manuscript with support from co-authors.

DISCLAIMERS & COMPETING INTERESTS

H.G. & J.F. have previously received travel and accommodation expenses to attend ONT conferences. The authors declare no other competing financial or non-financial interests.

Table 1. Sequencing accuracy for Illumina and ONT whole-genome sequencing of synthetic SARS-CoV-2 controls.

Illumina samples	Reportable (bp)	Read-level error rate (errors per base per read)				Erroneous variants			Consensus accuracy
		Total	Mismatch	Deletion	Insertion	Total	SNVs	Indels	
A	28687	0.00152	0.00083	0.00058	0.00011	0	0	0	100%
B	28687	0.00153	0.00082	0.00060	0.00012	0	0	0	100%
C	28687	0.00148	0.00079	0.00057	0.00012	0	0	0	100%
D	28687	0.00172	0.00098	0.00063	0.00011	0	0	0	100%
E	28687	0.00124	0.00089	0.00024	0.00011	0	0	0	100%
F	28687	0.00170	0.00137	0.00023	0.00011	0	0	0	100%
G	28687	0.00122	0.00088	0.00022	0.00011	0	0	0	100%
H	28687	0.00118	0.00084	0.00024	0.00011	0	0	0	100%
Mean	28687	0.00145	0.00092	0.00041	0.00011	0	0	0	100%

ONT samples	Reportable (bp)	Read-level error rate (errors per base per read)				Erroneous variants			Consensus accuracy
		Total	Mismatch	Deletion	Insertion	Total	SNVs	Indels	
A	28192	0.06067	0.02093	0.02475	0.01499	0	0	0	100%
B	28192	0.06180	0.02150	0.02527	0.01503	0	0	0	100%
C	28192	0.06114	0.02141	0.02476	0.01496	0	0	0	100%
D	28192	0.06110	0.02146	0.02471	0.01493	0	0	0	100%
E	28192	0.06013	0.02067	0.02445	0.01501	0	0	0	100%
F	28192	0.05972	0.02018	0.02457	0.01496	2	0	2	99.9929%
G	28192	0.06178	0.02173	0.02486	0.01520	0	0	0	100%
H	28192	0.06030	0.02049	0.02470	0.01511	0	0	0	100%
Mean	28192	0.06083	0.02105	0.02476	0.01502	0.25	0	0.25	99.9991%

Table 2. Consensus-level accuracy of ONT whole-genome SARS-CoV-2 sequencing on patient specimens.

*Blacklist sites are error-prone low-complexity sequences ($n = 15$; 9-42 bp; see text for details).

	Medaka	Medaka minus blacklist*	Nanopolish	Nanopolish minus blacklist*
Cases analysed	157	157	157	157
Genome coverage	99.59%	98.56%	99.59%	98.56%
Negative positions	4674554	4627768	4674554	4627768
<i>Illumina variants</i>	1201	1162	1201	1162
<i>ONT variants</i>	1190	1159	1196	1164
TPs	1181	1155	1191	1160
FNs	20	7	10	2
FPs	9	4	5	4
Sensitivity	98.33%	99.40%	99.17%	99.83%
Precision	99.24%	99.65%	99.58%	99.66%
Jaccard similarity	97.60%	99.06%	98.76%	99.49%
Perfect concordance	140/157 cases	149/157 cases	147/157 cases	152/157 cases
<i>Illumina SNVs</i>	1194	1162	1194	1162
<i>ONT SNVs</i>	1180	1155	1190	1160
TPs	1180	1155	1190	1160
FNs	14	7	4	2
FPs	0	0	0	0
Sensitivity	98.83%	99.40%	99.66%	99.83%
Precision	100%	100%	100%	100%
Jaccard similarity	98.83%	99.40%	99.66%	99.83%
Perfect concordance	145/157 cases	152/157 cases	153/157 cases	155/157 cases

Table 3. Detection of structural variation in SARS-CoV-2 specimens with ONT sequencing.

Specimen	SV type	Size	Position	Gene	Supporting ONT reads	Short-read evidence	Breakpoint resolution
kirby_nCoV_077	Deletion	15	18019-18034	orf1ab	94	yes	0,0
kirby_nCoV_087	Deletion	1132	1082-2214	orf1ab	48	no	.
kirby_nCoV_088	Deletion	34	26786-26820	M	75	yes	0,0
kirby_nCoV_106	Deletion	548	6004-6552	orf1ab	20	no	.
kirby_nCoV_125	Deletion	27	27263-27290	ORF6	20	yes	-2,-3
kirby_nCoV_183	Deletion	15	25533-25548	ORF3	41	yes	-2,-2
kirby_nCoV_214	Deletion	29	23554-23583	S	28	yes	+1, +2
kirby_nCoV_200	Deletion	328	27906-28234	ORF8	385	yes	0,0
kirby_nCoV_209	Deletion	639	2771-3410	orf1ab	48	yes	0,0
kirby_nCoV_211	Deletion	1840	509-2349	orf1ab	22	no	.
kirby_nCoV_225	Deletion	328	27906-28234	ORF8	387	yes	0,0
kirby_nCoV_235	Deletion	37	26783-26820	M	21	yes	+3,+4
kirby_nCoV_249	Deletion	702	2664-3366	orf1ab	52	yes	-1,0
kirby_nCoV_164	Deletion	588	22690-23278	S	59	yes	+1, +4
kirby_nCoV_083	Deletion	28	23554-23582	S	38	yes	0,0
kirby_nCoV_083	Deletion	13	29478-29491	N	36	yes	+1,+1

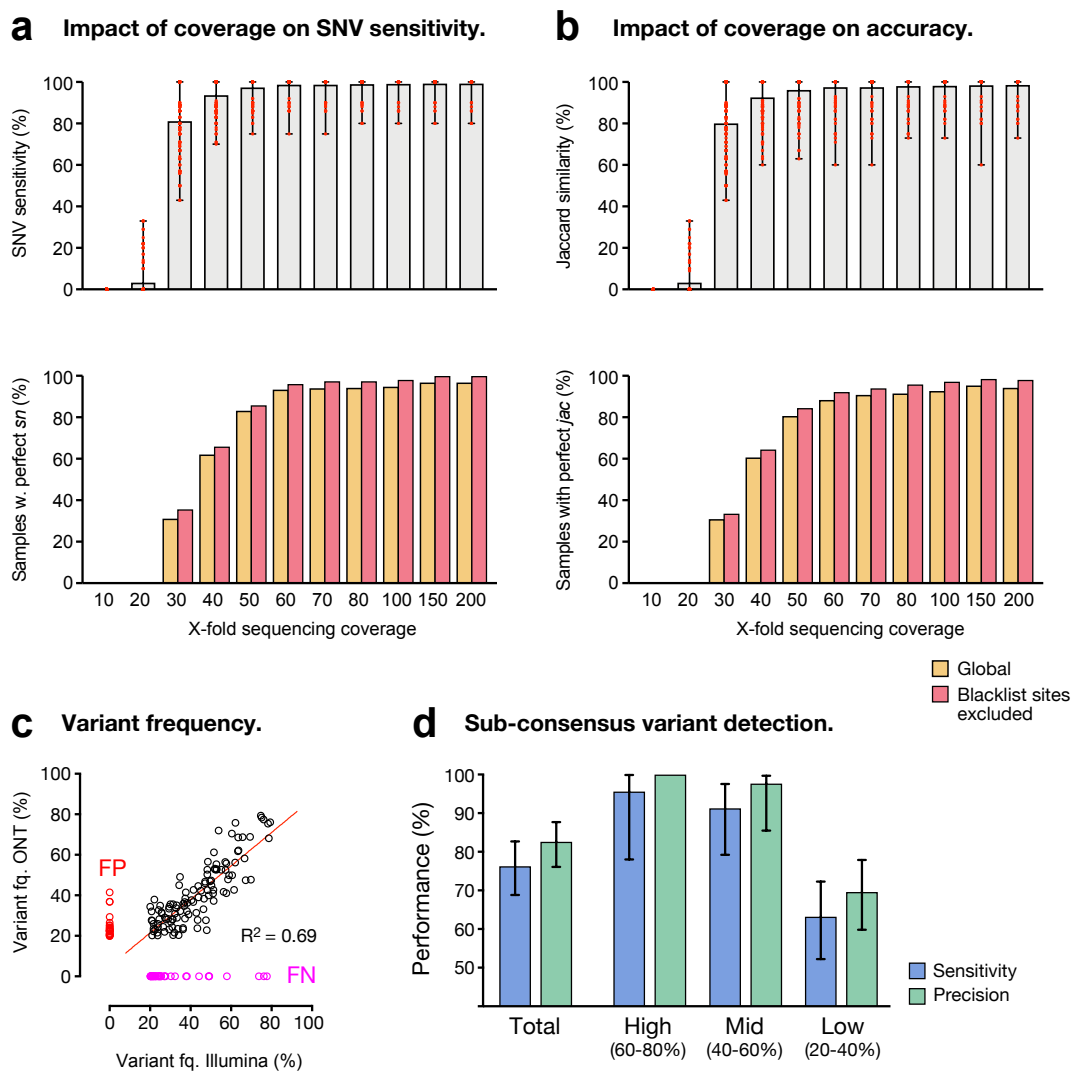


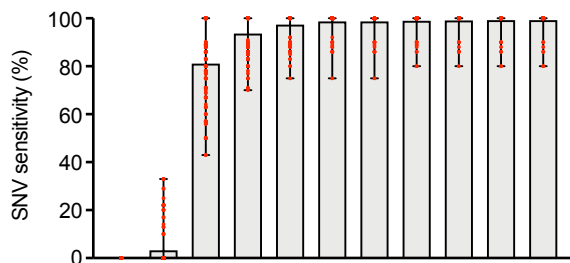
Fig. 1. Variant detection performance for whole-genome ONT sequencing of SARS-CoV-2. (a; upper) Sensitivity with which Illumina comparison SNVs at consensus-level variant frequencies (80-100%) were detected via ONT sequencing on matched SARS-CoV-2 specimens ($n = 157$). Bars show mean \pm range. (a; lower) Fraction of specimens tested in which SNVs were detected with perfect sensitivity (sn). Data are plotted separately for genome-wide variant detection (gold) and variant detection with error-prone 'blacklist' sites excluded (red). (b) Same as in a but Jaccard similarity (jac) scores for all variant candidates are plotted instead of SNV sn . (c) Correlation of variant frequencies observed for SNV candidates detected at sub-consensus frequencies (20-80%) with Illumina and ONT sequencing. Candidates detected with ONT but not Illumina were considered to be false-positives (FP; red) and candidates detected with Illumina but not ONT were considered to be false-negatives (FN; pink). (d) Sensitivity (blue) and precision (green) of SNV detection with ONT sequencing at sub-consensus variant frequencies (20-80%). Data are plotted separately for high (60-80%), intermediate (40-60%) and low (20-40%) frequencies. Error bars show 95% confidence intervals (Clopper-Pearson).

REFERENCES

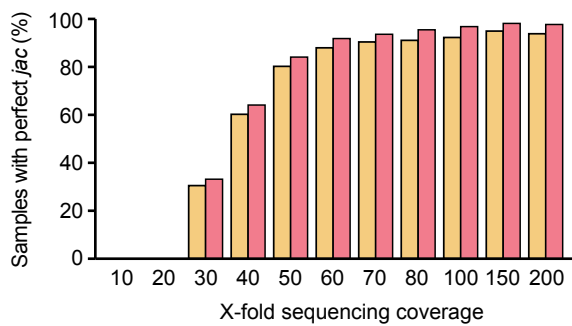
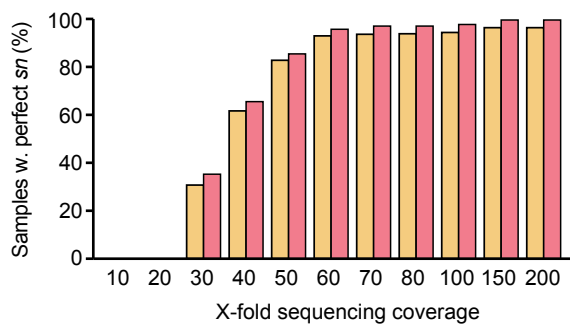
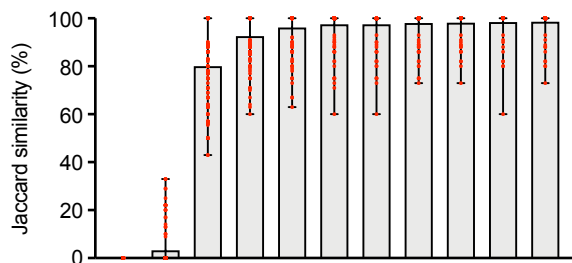
1. Wu, F. *et al.* A new coronavirus associated with human respiratory disease in China. *Nature* **579**, 265–269 (2020).
2. Zhu, N. *et al.* A Novel Coronavirus from Patients with Pneumonia in China, 2019. *N Engl J Med* **382**, 727–733 (2020).
3. Lu, R. *et al.* Genomic characterisation and epidemiology of 2019 novel coronavirus: implications for virus origins and receptor binding. *Lancet* **395**, 565–574 (2020).
4. van Kasteren, P. B. *et al.* Comparison of seven commercial RT-PCR diagnostic kits for COVID-19. *J Clin Virol* **128**, 104412 (2020).
5. Rambaut, A. *et al.* A dynamic nomenclature proposal for SARS-CoV-2 to assist genomic epidemiology. *bioRxiv* 2020.04.17.046086 (2020).
6. Eden, J.-S. *et al.* An emergent clade of SARS-CoV-2 linked to returned travellers from Iran. *Virus Evol* **6**, (2020).
7. Fauver, J. R. *et al.* Coast-to-coast spread of SARS-CoV-2 during the early epidemic in the United States. *Cell* **181**, 990–996.e5 (2020).
8. Gonzalez-Reiche, A. S. *et al.* Introductions and early spread of SARS-CoV-2 in the New York City area. *Science* eabc1917 (2020).
9. Gudbjartsson, D. F. *et al.* Spread of SARS-CoV-2 in the Icelandic population. *N Engl J Med* NEJMoa2006100 (2020). doi:10.1056/NEJMoa2006100
10. Lu, J. *et al.* Genomic epidemiology of SARS-CoV-2 in Guangdong province, China. *Cell* **181**, 997–1003.e9 (2020).
11. Rockett, R. J. *et al.* Revealing COVID-19 transmission in Australia by SARS-CoV-2 genome sequencing and agent-based modeling. *Nat Med* **26**, 1398–1404 (2020).
12. Korber, B. *et al.* Tracking changes in SARS-CoV-2 Spike: evidence that D614G increases infectivity of the COVID-19 virus. *Cell* (2020).
13. Li, Q. *et al.* The impact of mutations in SARS-CoV-2 spike on viral infectivity and antigenicity. *Cell* (2020).
14. Uddin, M. *et al.* SARS-CoV-2/COVID-19: Viral Genomics, Epidemiology, Vaccines, and Therapeutic Interventions. *Viruses* **12**, (2020).
15. Young, B. E. *et al.* Effects of a major deletion in the SARS-CoV-2 genome on the severity of infection and the inflammatory response: an observational cohort study. *Lancet* **396**, 603–611 (2020).
16. Jain, M., Olsen, H. E., Paten, B. & Akeson, M. The Oxford Nanopore MinION: delivery of nanopore sequencing to the genomics community. *Genome Biol* **17**, 239 (2016).
17. Quick, J. *et al.* Rapid draft sequencing and real-time nanopore sequencing in a hospital outbreak of Salmonella. *Genome Biol* **16**, 114 (2015).
18. Quick, J. *et al.* Real-time, portable genome sequencing for Ebola surveillance. *Nature* **530**, 228–232 (2016).
19. Quick, J. *et al.* Multiplex PCR method for MinION and Illumina sequencing of Zika and other virus genomes directly from clinical samples. *Nat Protoc* **12**, 1261–1276 (2017).
20. Meredith, L. W. *et al.* Rapid implementation of SARS-CoV-2 sequencing to investigate cases of health-care associated COVID-19: a prospective genomic surveillance study. *The Lancet Infectious Diseases* (2020). doi:10.1016/S1473-3099(20)30562-4
21. Paden, C. *et al.* Rapid, sensitive, full-genome sequencing of Severe Acute Respiratory Syndrome Coronavirus 2. *Emerging Infectious Disease journal* **26**, (2020).
22. Walker, A. *et al.* Genetic structure of SARS-CoV-2 reflects clonal superspreading and multiple independent introduction events, North-Rhine Westphalia, Germany, February and March 2020. *Euro Surveill* **25**, (2020).
23. Rang, F. J., Kloosterman, W. P. & de Ridder, J. From squiggle to basepair: computational approaches for improving nanopore sequencing read accuracy. *Genome Biol* **19**, 90 (2018).
24. Tyler, A. D. *et al.* Evaluation of Oxford Nanopore's MinION sequencing device for microbial whole genome sequencing applications. *Sci Rep* **8**, 10931 (2018).

25. Laver, T. *et al.* Assessing the performance of the Oxford Nanopore Technologies MinION. *Biomol Detect Quantif* **3**, 1–8 (2015).
26. Rambaut, A. *Phyldynamic Analysis / 176 genomes / 6 Mar 2020. virological.org* (2020).
27. Hardwick, S. A., Deveson, I. W. & Mercer, T. R. Reference standards for next-generation sequencing. *Nat Rev Genet* **18**, 473–484 (2017).
28. Henn, M. R. *et al.* Whole genome deep sequencing of HIV-1 reveals the impact of early minor variants upon immune recognition during acute infection. *PLoS Pathog* **8**, e1002529 (2012).
29. Vignuzzi, M., Stone, J. K., Arnold, J. J., Cameron, C. E. & Andino, R. Quasispecies diversity determines pathogenesis through cooperative interactions in a viral population. *Nature* **439**, 344–348 (2006).
30. Stern, A. *et al.* The evolutionary pathway to virulence of an RNA virus. *Cell* **169**, 35–46.e19 (2017).
31. Worby, C. J., Lipsitch, M. & Hanage, W. P. Shared genomic variants: identification of transmission routes using pathogen deep-sequence data. *Am J Epidemiol* **186**, 1209–1216 (2017).
32. De Maio, N., Worby, C. J., Wilson, D. J. & Stoesser, N. Bayesian reconstruction of transmission within outbreaks using genomic variants. *PLoS Comput Biol* **14**, e1006117–e1006117 (2018).
33. Wymant, C. *et al.* PHYLOSCANNER: Inferring transmission from within- and between-host pathogen genetic diversity. *Mol Biol Evol* **35**, 719–733 (2018).
34. Gong, Y.-N. *et al.* SARS-CoV-2 genomic surveillance in Taiwan revealed novel ORF8-deletion mutant and clade possibly associated with infections in Middle East. *Emerging Microbes & Infections* **9**, 1457–1466 (2020).
35. Samarakoon, H. *et al.* Genopo: a nanopore sequencing analysis toolkit for portable Android devices. *Communications Biology* **3**, 538 (2020).
36. Li, H. & Durbin, R. Fast and accurate short read alignment with Burrows–Wheeler transform. *Bioinformatics* **25**, 1754–1760 (2009).
37. Grubaugh, N. D. *et al.* An amplicon-based sequencing framework for accurately measuring intrahost virus diversity using PrimalSeq and iVar. *Genome Biol* **20**, 8 (2019).
38. Li, H. A statistical framework for SNP calling, mutation discovery, association mapping and population genetic parameter estimation from sequencing data. *Bioinformatics* **27**, 2987–2993 (2011).
39. Mapleson, D., Drou, N. & Swarbreck, D. RAMPART: a workflow management system for de novo genome assembly. *Bioinformatics* **31**, 1824–1826 (2015).
40. Li, H. Minimap2: pairwise alignment for nucleotide sequences. *Bioinformatics* **34**, 3094–3100 (2018).
41. Simpson, J. T. *et al.* Detecting DNA cytosine methylation using nanopore sequencing. *Nat Methods* **14**, 407–410 (2017).
42. Edge, P. & Bansal, V. Longshot enables accurate variant calling in diploid genomes from single-molecule long read sequencing. *Nat Commun* **10**, 4660 (2019).
43. Koboldt, D. C. *et al.* VarScan 2: somatic mutation and copy number alteration discovery in cancer by exome sequencing. *Genome Res* **22**, 568–576 (2012).
44. Sedlazeck, F. J. *et al.* Accurate detection of complex structural variations using single-molecule sequencing. *Nat Methods* **15**, 461–468 (2018).
45. Layer, R. M., Chiang, C., Quinlan, A. R. & Hall, I. M. LUMPY: a probabilistic framework for structural variant discovery. *Genome Biol* **15**, R84 (2014).

a Impact of coverage on SNV sensitivity.



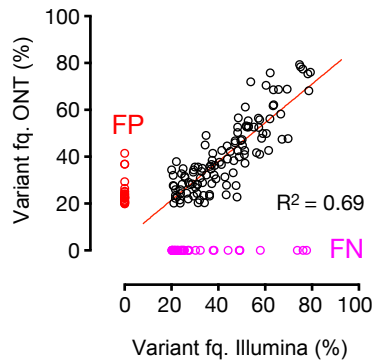
b Impact of coverage on accuracy.



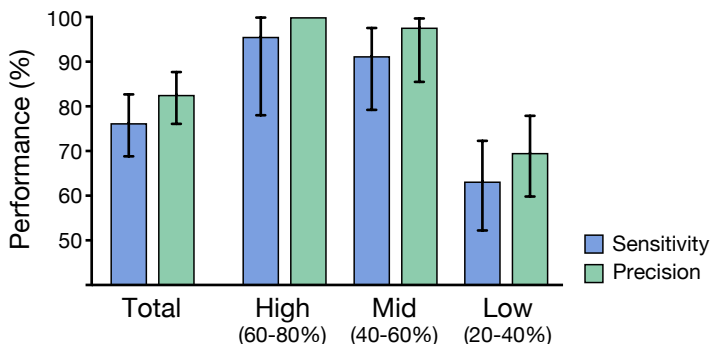


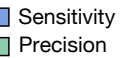
 Global
 Blacklist sites excluded

c Variant frequency.



d Sub-consensus variant detection.





 Sensitivity
 Precision